Journal of Biosciences and Medicines, 2015, 3, 1-6
Published Online December 2015 in SciRes. http://www.scirp.org/journal/jbm
http://dx.doi.org/10.4236/jbm.2015.312001

Transgenic Mouse (Tg2576) Is an Ideal Model for the Biological Characterization of [^{18}F]-FDDNP for Identifying Alzheimer's Disease

Kang-Wei Chang*, Shih-Ying Lee, Chia-Chieh Chen

Division of Isotope Application, Institute of Nuclear Energy Research, Taiwan
Email: *kwchang@iner.gov.tw

Received 8 October 2015; accepted 11 December 2015; published 18 December 2015

Abstract

[^{18}F]-FDDNP was synthesized and characterized as a positron-emitting probe to identify Alzheimer's disease (AD) in transgenic mouse models (Tg2576 and dE9) expressing the AD pathology. We observed in *in vitro*, *in vivo*, and *ex vivo* studies that [^{18}F]-FDDNP accumulated specifically in the Aβ-overexpressing brain regions and that this accumulation was significantly reduced by co-incubation with non-radioactive FDDNP. In *ex vivo* and *in vivo* studies of brain sections, the retention of radioactivity was more specific in Tg2576 mice than in dE9 mice. Using *in vitro*, *ex vivo*, *in vivo*, and ELISA analyses, we characterized the utility of [^{18}F]-FDDNP in mapping β-amyloid in the Tg2576 mouse brain, to assess its potential application in imaging strategies.

Keywords

[^{18}F]-FDDNP, Alzheimer's Disease, Transgenic Mice, β-Amyloid Plaques

1. Introduction

Alzheimer's disease (AD) is the most common neurodegenerative brain disease, and it is characterized by memory impairment and a broad spectrum of cognitive deficits, including progressive memory loss and declining cognitive functions [1] [2].

The clinical diagnosis of AD has severe limitations and, importantly, the disease is already advanced by the time it is definitively diagnosed [3] [4]. Highly quantitative imaging methods with high resolution, high selectivity, and high definition of detailed biological required for neurodegenerative and psychiatric disease research [5] [6].

2-(1-{6-[(2-[^{18}F]-Fluoroethyl)(methyl)amino]-2-naphthyl}ethylidene)malononitrile ([^{18}F]-FDDNP), developed at the University of California, Los Angeles (UCLA), has previously been used to label neuropathology materials (senile plaques and neurofibrillary tangles, hallmark lesions of the AD brain) in the living brains of

*Corresponding author.

How to cite this paper: Chang, K.-W., Lee, S.-Y. and Chen, C.-C. (2015) Transgenic Mouse (Tg2576) Is an Ideal Model for the Biological Characterization of [^{18}F]-FDDNP for Identifying Alzheimer's Disease. *Journal of Biosciences and Medicines*, **3**, 1-6.
http://dx.doi.org/10.4236/jbm.2015.312001

AD patients for PET analysis [1] [2].

Laboratory animals with a marker of the disease are very useful in determining the pathogenesis of AD and identifying promising treatments [7]. Numerous models have successfully replicated amyloid plaque deposition and the inclusion of a mutant presenilin (*PSEN1*) allele can accelerate the deposition rate and exacerbate the pathological severity of the disease [1] [8].

To further characterize the binding properties of [^{18}F]-FDDNP in transgenic rodents, we extended APP transgenic mouse (Tg2576) and the PS/APP double-transgenic mouse (dE9), which express AD. The results of our studies of [^{18}F]-FDDNP used *in vitro* and *ex vivo* and with microPET imaging to predict the pathogenic processes of AD and provide a standard diagnostic method for this disease.

2. Materials and Methods

2.1. Chemicals

The precursor of FDDNP was purchased from ABX (Radeberg, Germany). Acetic anhydride, 30% hydrogen peroxide, potassium iodide, dimethyl sulfoxide, potassium carbonate, ethylene glycol, anhydrous acetonitrile were purchased from Merck & Co., Inc. (Whitehouse Station, NJ, USA).

2.2. Animal Models

14 - 16-month-old transgenic Tg2576 and dE9 mice expressing mutated human APP and APP/PS1 proteins, respectively. All animal procedures and experimental protocols were approved by the Ethical Animal Use Committee of the Institute of Nuclear Energy Research (INER), Taiwan.

2.3. Synthesis of [^{18}F]-FDDNP

FDDNP was prepared according to the procedure published in 2007 [9].

2.4. *In Vitro* and *ex Vivo* Autoradiography

Tg2576, dE9, and control mice aged 14 - 16 months were anaesthetized with isoflurane gas (1 mL per minute) and injected with 185 MBq/200 μL [^{18}F]-FDDNP through their lateral tail veins. Each group were killed by decapitation 30 min after injection. Their brains were immediately removed and frozen in powered dry ice. Sagittal sections of 20 μm cut and exposed to Kodak XAR film for 72 h.

2.5. MicroPET Imaging and Data Analysis

Mice were injected with about 18.5 MBq of [^{18}F]-FDDNP via the lateral tail vein. After distributed for 30 min, placed inside the microPET-R4® system (Concorde Microsystems, Knoxville, TN, USA) for tomographic imaging (10 min). AsiPro software (Concorde Microsystems) was used for the statistical analysis; a region of interest (ROI) was defined in each brain region.

2.6. Human Amyloid β(1 - 40) Enzyme-Linked Immunosorbent Assay (ELISA)

Mice were killed with carbon dioxide. Distinguishable regions (olfactory bulb, cortex, striatum, thalamus, hypothalamus, midbrain, cerebellum, Pons, and medulla) were transferred to polypropylene tubes and each sonicated sample was clarified for human amyloid β(1 - 40) ELISA Kit IBL code no. 27,713 (Immuno-Biological Laboratories Co., Ltd, Fujioka, Japan), according to the manufacturer's protocols.

3. Results and Discussion

[^{18}F]-FDDNP was developed in 2001 in Dr Barrio's laboratory at UCLA [10]. It has shown excellent results with AD in transgenic rats and patients *in vivo* and *in vitro* analyses [10] [11]. The lipophilic characteristic of [^{18}F]-FDDNP (1.93 ± 0.10) which was indicated high lipophilicity and suggested could penetrate the BBB.

The results of *in vitro* autoradiography and a competition assay (**Figure 1** and **Table 1**) demonstrate the high binding capacity and specificity of FDDNP in the Tg2576 transgenic mouse. In the Aβ-rich brain regions (hippocampus and frontal cortex), the dE9 mice also displayed significantly higher binding than the normal mice

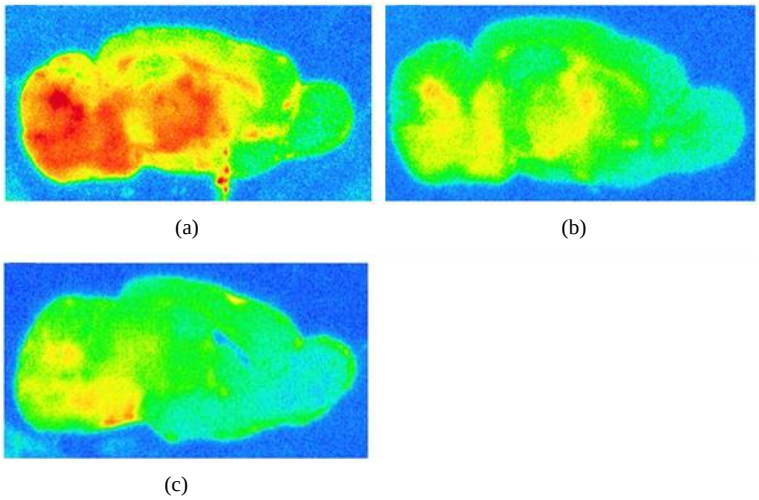

(a) (b)

(c)

Figure 1. Brain autoradiography of transgenic mice ((a) Tg2576; (b) dE9) and normal mice (c) after incubation with [18F]-FDDNP.

Table 1. The binding of [^{18}F]-FDDNP, in different brain regions, derived from the brain autoradiograms shown in **Figure 1**, for the Tg2576 and dE9 transgenic mice and the competition assay groups treated with 20 or 200 μg of FDDNP carrier (n = 3, means ± SD).

Brain region	Tg2576 mice			dE9 mice			Normal mice		
	n.c.a.[a] [^{18}F]FDDNP	20 μg FDDNP carrier	200 μg FDDNP carrier	n.c.a. [^{18}F]FDDNP	200 μg FDDNP carrier	20 μg FDDNP carrier	n.c.a. [^{18}F]FDDNP	20 μg FDDNP carrier	200 μg FDDNP carrier
Cortex	109.79 ± 25.33	87.52 ± 22.48	33.92 ± 11.98*	27.41 ± 4.47°	6.63 ± 1.87*	4.77 ± 2.04*	7.19 ± 1.81	5.63 ± 0.73	2.44 ± 0.57
Hippocampus	49.15 ± 13.50^{+}	34.16 ± 11.40	23.31 ± 9.30	8.71 ± 4.02	2.00 ± 1.08	1.65 ± 0.76	4.05 ± 1.04	4.74 ± 1.54	2.14 ± 1.08
Thalamus	73.07 ± 16.73^{+}	28.94 ± 14.06*	17.75 ± 8.78*	9.73 ± 1.89	1.37 ± 0.39*	2.65 ± 1.02*	9.54 ± 1.98	4.52 ± 1.57*	10.33 ± 3.00
Hypothalamus	44.14 ± 15.02^{+}	32.31 ± 8.02	19.44 ± 8.19*	8.25 ± 0.76	1.20 ± 0.84*	1.26 ± 0.78*	5.87 ± 1.20	4.35 ± 1.93	4.06 ± 1.27
Midbrain	39.39 ± 13.99^{+}	28.51 ± 10.68	20.54 ± 0.76	6.72 ± 3.61	0.90 ± 0.34	3.82 ± 1.91	1.26 ± 1.14	8.36 ± 1.65*	2.43 ± 1.51
Pons	38.28 ± 15.53	24.97 ± 7.24	20.08 ± 11.06*	6.00 ± 2.04	1.87 ± 0.91*	0.02 ± 0.01*	5.43 ± 1.99	10.17 ± 4.98	3.50 ± 1.42
Medulla	38.61 ± 13.67^{+}	28.57 ± 8.97	23.43 ± 13.96	8.33 ± 1.70	1.63 ± 1.01*	3.23 ± 1.20*	9.55 ± 2.83	1.49 ± 0.74	0.17 ± 0.10*
Cerebellum	115.50 ± 33.25	110.78 ± 27.45	48.93 ± 16.63	22.01 ± 13.54	12.36 ± 6.59	11.44 ± 4.24	22.70 ± 6.34	3.49 ± 1.59*	21.89 ± 12.11

[a] n.c.a: not-carrier-added. $^{*}P < 0.05$, student's *t* test, for comparison within brain region and tracer, between carrier addition. $^{+}P < 0.05$, for comparison within Tg2576 mice brain region between dE9 and normal mice. $^{\circ}P < 0.05$, for comparison with brain region between dE9 and normal mice.

($p < 0.01$). Immunohistochemical staining of the Tg2576 mouse brains also identified high levels of Aβ protein in the hippocampus and frontal cortex (data not shown). We noted that in the Tg2576 mice, [^{18}F]-FDDNP accumulated strongly in the cerebellum, may be inferred that the overexpression of APP protein and the accumulation of Aβ plaques in the cerebellum [1] [4].

In the competition study, [^{18}F]-FDDNP binding was inhibited by co-incubation with the carrier (**Table 1**). More [^{18}F]-FDDNP accumulated in the Tg2576 brain than in the dE9 and normal mouse brains, and was not comprehensive among the brain regions.

Ex vivo autoradiography was also used to compare the binding of [^{18}F]-FDDNP to the Aβ-rich regions in the transgenic and normal mice (**Figure 2** and **Table 2**). The Tg2576 mice showed significant differences from the dE9 mice in the binding of [^{18}F]-FDDNP in the thalamus, midbrain, and medulla, and significant differences from the normal mice in the thalamus, midbrain, medulla, and cerebellum [3]. Although the data presented show only a few significant differences in the brain regions of the transgenic mice, our results are similar to those published by Kung *et al.* [12]. MicroPET imaging was performed 30 min after the injection of [^{18}F]-FDDNP (18.5 MBq). The signal quantified in the ROIs in these transverse sections compare with the reference baseline

indicated ratios of 0.84 - 1.00 relative to muscle in the Tg2576 mice (**Table 3**). When the radioactive signal of [^{18}F]-FDDNP was calculated relative to the same reference (muscle) in the dE9 transgenic mice, the ratios for different brain regions were 0.10 - 0.32 (**Table 3**). The specific binding ratios in whole brain regions showed greater accumulation of [^{18}F]-FDDNP in the Tg2576 mice than in the dE9 or normal mice (**Figure 3**). The immunoreactivity of human amyloid β(1 - 40) was quantified in the olfactory bulb, cortex, striatum, thalamus, hypothalamus, midbrain, cerebellum, pons, and medulla. A standard curve was constructed for human Aβ protein, ranging from 500 pg/mL to 7.813 pg/mL, and the linear standard curve equation was derived for continuous analysis (R2 = 0.995 - 0.998). In the Tg2576 mice, the amount of human β-amyloid in the whole brain (0.257 - 1.992 ng/mL) was significantly different from the amounts in the dE9 (0.085–0.567 ng/mL) and normal mouse brains (0.031 - 0.098 ng/mL) (**Table 4**). The present study suggests that [^{18}F]-FDDNP has excellent potential

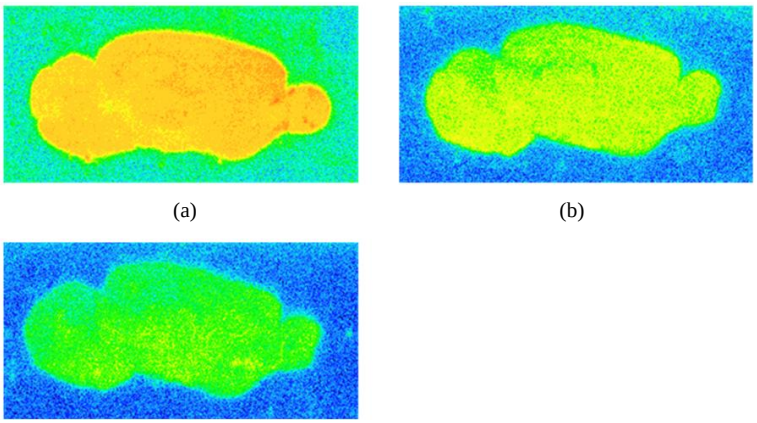

(a) (b)

(c)

Figure 2. *Ex vivo* brain autoradiography of transgenic mice ((a) Tg2576; (b) dE9) and normal mice (c) 30 min after injection with 185 MBq/200 μL [18F]-FDDNP.

Table 2. The binding densities of [^{18}F]-FDDNP in different brain regions of the Tg2576 and dE9 transgenic mice and normal mice, derived from *ex vivo* brain autoradiograms (n = 3, mean ± SD).

	Tg2576	dE9	Normal mice
Cortex	48.21 ± 28.09	29.72 ± 15.83	10.93 ± 8.07
Hippocampus	48.48 ± 24.58	35.54 ± 16.64	13.97 ± 7.11
Thalamus	51.53 ± 19.16*	36.80 ± 17.91	12.54 ± 6.76°
Hypothalamus	41.36 ± 19.90	31.79 ± 13.82	10.94 ± 3.79
Midbrain	54.40 ± 16.05*	44.61 ± 15.06^{+}	16.52 ± 8.16°
Pons	61.50 ± 25.09	35.74 ± 17.47	15.15 ± 6.48
Medulla	74.67 ± 24.26*	31.90 ± 9.31^{+}	13.81 ± 6.55°
Cerebellum	54.28 ± 18.15	33.77 ± 7.06^{+}	14.29 ± 6.87°

$^{*}P < 0.05$, student's *t* test, for comparison within brain region and tracer, between Tg2576 and dE9 mice. $^{+}P < 0.05$, for comparison within dE9 and normal mice. $^{\circ}P < 0.05$, for comparison with Tg2576 and normal mice.

Table 3. Specific binding ratios for different brain regions (olfactory bulb, cortex, striatum, thalamus, and cerebellum) of the Tg2576 and dE9 transgenic mice and normal mice relative to that in muscle from the head region, derived from *in vivo* microPET images (n = 3, mean ± SD).

Specific binding ratio	Olfactory bulb	Cortex	Striatum	Thalamus	Cerebellum
Tg2576	0.90 ± 0.33*	0.91 ± 0.28°	1.00 ± 0.34$^{*\circ}$	1.00 ± 0.27$^{*\circ}$	0.84 ± 0.14$^{*\circ}$
dE9	0.31 ± 0.17	0.22 ± 0.11	0.12 ± 0.07	0.10 ± 0.05	0.32 ± 0.11^{+}
Normal mice	0.20 ± 0.14	0.19 ± 0.09	0.08 ± 0.02	0.07 ± 0.01	0.06 ± 0.02

$^{*}P < 0.05$, student's *t* test, for comparison within brain region and tracer, between Tg2576 and dE9 mice. $^{+}P < 0.05$, for comparison within dE9 and normal mice. $^{\circ}P < 0.05$, for comparison with Tg2576 and normal mice.

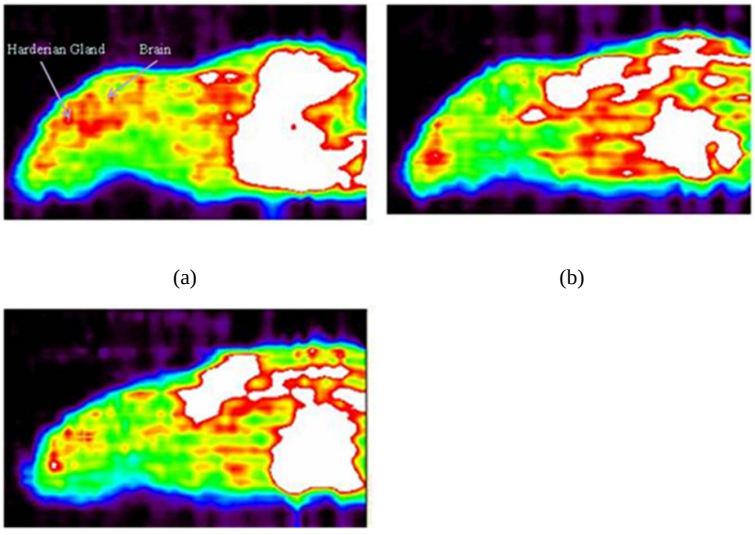

(a) (b)

(c)

Figure 3. *In vivo* microPET imaging of the accumulation of [18F]-FDDNP in brain sections 30 min post-injection into Tg2576 (a); dE9 (b); and normal mice (c).

Table 4. Levels of immunoreactivity for human amyloid β(1 - 40) in supernatants derived from different brain sections (olfactory bulb, cortex, striatum, thalamus, hypothalamus, midbrain, cerebellum, pons, and medulla) were quantified by ELISA using a human Aβ assay kit (n = 3, mean ± SD).

ng/ml	Tg2576	dE9	Normal mice
Olfactory bulb	$1.992 \pm 0.015^{*\circ}$	$0.171 \pm 0.046^{+}$	0.031 ± 0.003
Cortex	$1.984 \pm 0.026^{*\circ}$	0.567 ± 0.016	0.098 ± 0.005
Striatum	$1.931 \pm 0.007^{*\circ}$	0.378 ± 0.086	0.031 ± 0.002
Thalamus	$0.257 \pm 0.017^{\circ}$	$0.311 \pm 0.018^{+}$	0.031 ± 0.001
Hypothalamus	$0.386 \pm 0.004^{*\circ}$	$0.293 \pm 0.029^{+}$	0.030 ± 0.002
Midbrain	$0.068 \pm 0.003^{*\circ}$	$0.098 \pm 0.008^{+}$	0.036 ± 0.001
Cerebellum	$1.232 \pm 0.018^{*\circ}$	$0.142 \pm 0.067^{+}$	0.038 ± 0.001
Pons and medulla	$0.078 \pm 0.008^{\circ}$	$0.085 \pm 0.011^{+}$	0.039 ± 0.001

$^{*}P < 0.05$, student's *t* test, for comparison within brain region and tracer, between Tg2576 and dE9 mice. $^{+}P < 0.05$, for comparison within dE9 and normal mice. $^{\circ}P < 0.05$, for comparison with Tg2576 and normal mice.

utility in Tg2576 mice, but not in dE9 mice, and that this correlates with the amounts of Aβ protein in their brains.

References

[1] Newberg, A.B., Wintering, N.A., Plössl, K., Hochold, J., Stabin, M.G., Watson, M., Skovronsky, D., Clark, C.M., Kung, M.P. and Kung, H.F. (2006) Safety, Biodistribution, and Dosimetry of 123I-IMPY: A Novel Amyloid Plaque-Imaging Agent for the Diagnosis of Alzheimer's Disease. *J Nucl Med.*, **47**, 748-754.

[2] Reiman, E.M., Uecker, A., Gonzalez-Lima, F., Minear, D., Chen, K., Callaway, N.L., Berndt, J.D. and Games, D. (2000) Tracking Alzheimer's Disease in Transgenic Mice Using Fluorodeoxyglucose Autoradiography. *Neuroreport*, **11**, 987-991. http://dx.doi.org/10.1097/00001756-200004070-00018

[3] Lee, C.W., Kung, M.P., Hou, C. and Kung, H.F. (2003) Dimethylamino-Fluorenes: Ligands for Detecting β-Amyloid Plaques in the Brain. *Nucl Med Biol.*, **30**, 573-580. http://dx.doi.org/10.1016/S0969-8051(03)00050-7

[4] Nakamura, S., Murayama, N., Noshita, T., Annoura, H. and Ohno, T. (2001) Progressive Brain Dysfunction Following

Intracerebroventricular Infusion of Beta1-42-Amyloid Peptide. *Brain Res.*, **912**, 128-136. http://dx.doi.org/10.1016/S0006-8993(01)02704-4

[5] Lockhart, A. (2006) Imaging Alzheimer's Disease Pathology: One Target, Many Ligands. *Drug Discov Today*, **11**, 1093-1099. http://dx.doi.org/10.1016/j.drudis.2006.10.008

[6] Routtenberg, A. (1997) Measuring Memory in a Mouse Model of Alzheimer's Disease. *Science*, **277**, 839-841. http://dx.doi.org/10.1126/science.277.5327.839

[7] Barrios, J.R., Kepea, V., Satyamurthy, N., Huang, S.C. and Gary, W. (2006) Brain Pathology and Neuronal Losses in the Living Brain of Alzheimer's Patients. *Int Congr Ser.*, **1290**, 150-155. http://dx.doi.org/10.1016/j.ics.2005.11.102

[8] Giovannelli, L., Casamenti, F., Scali, C., Bartolini, L. and Pepeu, G. (1995) Differential Effects of Amyloid Peptides β-(1-40) and β-(25-35) Injections into the Rat Nucleus Basalis. *Neuroscience*, **66**, 781-792. http://dx.doi.org/10.1016/0306-4522(94)00610-H

[9] Liu, J., Kepe, V., Zabjek, A., Petric, A., Padgett, H.C., Satyamurthy, N. and Barrio, J.R. (2007) High-Yield, Automated Radiosynthesis of 2-(1-{6-[(2-[18F]Fluoroethyl)(methyl)amino]-2-naphthyl}ethylidene)malononitrile ([18F]FDDNP) Ready for Animal or Human Administration. *Mol Imaging Biol.*, **9**, 6-16. http://dx.doi.org/10.1007/s11307-006-0061-4

[10] Agdeppa, E.D., Kepe, V., Liu, J., Flores-Torres, S., Satyamurthy, N., Petric, A., Cole, G.M., Small, G.W., Huang, S.C. and Barrio, J.R. (2001) Binding Characteristics of Radiofluorinated 6-Dialkylamino-2-Naphthylethylidene Derivatives as Positron Emission Tomography Imaging Probes for β-Amyloid Plaques in Alzheimer's Disease. *J Neurosci.*, **21**, RC189.

[11] Agdeppa, E.D., Kepe, V., Liu, J., Small, G.W., Huang, S.C., Petric, A., Satyamurthy, N. and Barrio, J.R. (2003) 2-Dialkylamino-6-acylmalononitrile Substituted Naphthalenes (DDNP Analogs): Novel Diagnostic and Therapeutic Tools in Alzheimer's Disease. *Mol Imaging Biol.*, **5**, 404-417. http://dx.doi.org/10.1016/j.mibio.2003.09.010

[12] Kung, H.F., Kung, M.P., Zhuang, Z.P., Hou, C., Lee, C.W., Plössl, K., Zhuang, B., Skovronsky, D.M., Lee, V.M. and Trojanowski, J.Q. (2003) Iodinated Tracers for Imaging Amyloid Plaques in the Brain. *Mol Imaging Biol.*, **5**, 418-426. http://dx.doi.org/10.1016/j.mibio.2003.09.003